RSC Advances

PAPER

View Article Online
View Journal | View Issue

Cite this: *RSC Adv.*, 2017, **7**, 55905

Highly efficient removal of hexavalent chromium in aqueous solutions *via* chemical reduction of plate-like micro/nanostructured zero valent iron†

Shenghong Kang,[ab] Guozhong Wang,[a] Huijun Zhao[a] and Weiping Cai*[ab]

The removal of hexavalent chromium [Cr(VI)] from aqueous solutions using plate-like micro/nanostructured zero valent iron (MNZVI), which is fabricated in mass production by ball-milling of reductive iron powders, is investigated in this study. It has been shown that this plate-like MNZVI has significantly enhanced ability to remove Cr(VI) from aqueous solutions as compared to commercial zero valent iron (CZVI). Cr(VI) in a concentration of 100 ppm at pH = 2 can be removed nearly completely within 20 min by the addition of 1.5 g L^{-1} MNZVI. The time-dependent removal amount of Cr(VI) can be well described by a pseudo first-order kinetic model. The reaction rate constant for MNZVI is 20 times larger than that for CZVI. Further experiments have revealed that the Cr(VI) removal is also associated with the pH value and initial concentration of Cr(VI) in the solution, in addition to the iron dosage. These enhanced removal performances are attributed to the iron-induced reduction process of Cr(VI) and the high specific surface area of MNZVI. Further, electroplating wastewater was used to demonstrate the practical applications of MNZVI. The removal capacity is up to 330 mg g^{-1} in the electroplating wastewater with a 556 ppm initial Cr(VI) content, which is more than 3 times higher than that of CZVI and also much higher than the previously reported results. This study has demonstrated that the ball milling-induced plate-like MNZVI is a good candidate material for efficient treatment of Cr(VI)-containing wastewater.

Received 1st October 2017
Accepted 26th November 2017

DOI: 10.1039/c7ra10846j

rsc.li/rsc-advances

1. Introduction

In recent years, heavy metal pollution has been regarded as a serious threat since it has pervaded many parts of the world, especially the developing countries such as China.[1–3] Chromium (Cr) is one of the main heavy metal pollutants with a high toxicity and widely used in industries such as metal electroplating, leather tanning, and corrosion protection. Chromium has usually two stable oxidation states in aqueous solutions: hexavalent [Cr(VI)] and trivalent [Cr(III)].[4] Cr(VI) usually exists in the forms of chromate (CrO_4^{2-} or $HCrO_4^-$) and dichromate ($Cr_2O_7^{2-}$) depending on the pH value in solutions and has high mobility in subsurface water.[5] Cr(VI) pollution can increase the risk of catching dermatitis, rhinitis, and even cancer.[6] Many methods, such as physicochemical adsorption,[7] bioremediation,[6] chemical reduction,[8] precipitation,[9] membrane separation,[10] and ion exchange,[11] have been developed to remediate Cr(VI) contamination. Among them, physicochemical adsorption is an efficient way to remove Cr(VI). For instance, Naghizadeh *et al.* found that the capacities of carbon nanotubes and activated carbon to adsorb Cr(VI) were 4.5 mg g^{-1} and 2.4 mg g^{-1}, respectively.[12] However, the cost of this method is relatively high, and Cr(VI) is only transferred to another place instead of being eliminated.[13] Moreover, Cr(VI) is easily dissolved in aqueous solutions and hard to be adsorbed by common adsorbents. Bioremediation can effectively degrade Cr(VI) with low cost, but the micro-organisms used are limited and easily die due to the presence of bactericidal toxicants at many waste sites.[6] The chemical reduction method can be used to remove Cr(VI) rapidly and effectively using a reducing agent such as ferrous sulfate, sulfur dioxide, or sodium bisulfate.[14] However, it is severely restricted because of the relatively expensive reducing agents and complicated process.

Contrary to Cr(VI), Cr(III) has low toxicity and low solubility and can be easily hydrolyzed into $Cr(OH)_3$, which can expediently be separated from water.[15–17] Reduction from Cr(VI) to Cr(III) has been a hopeful and economic way to reduce the toxicity of Cr. Among various reductants, zero-valent iron (ZVI) is a strong reducer and has received wide attention in the past 20 years.[18,19] ZVI has a long history in the electronic and chemical industries due to its magnetic properties and high reaction activity.[20] Currently, ZVI has become one of the most popular materials for the removal of poisonous and harmful

[a]*Key Laboratory of Materials Physics, Anhui Key Laboratory of Nanomaterials and Nanotechnology, Center for Environmental and Energy Nanomaterials, Institute of Solid State Physics, Chinese Academy of Sciences, Hefei 230031, P. R. China. E-mail: wpcai@issp.ac.cn*

[b]*Department of Materials Science and Engineering, University of Science and Technology of China, Hefei 230026, P. R. China*

† Electronic supplementary information (ESI) available. See DOI: 10.1039/c7ra10846j

pollutants in contaminated soils and ground waters.[21,22] Specifically, ZVI nanoparticles have a large specific surface area and can be used for the treatment of recalcitrant environmental pollutants, as extensively reported in literature.[23,24] There have also been some reports on Cr(VI) removal by ZVI nanoparticles.[5,25,26] For instance, Wang *et al.*[25] reported Cr(VI) removal by ZVI nanoparticles in an aqueous solution with humic acid. About 75% Cr(VI) could be removed within 30 min from the solution with 20 ppm initial Cr(VI) content after the addition of ZVI nanoparticles (0.3 g L^{-1}) and humic acid (5 mg L^{-1}). Fang *et al.*[27] found that nanoscaled ZVI removes Cr(VI) *via* reduction immobilization of chromium and has a Cr(VI) removal capacity of about 182 mg g^{-1} in electroplating wastewater with pH = 4.82. However, the ZVI nanoparticles easily aggregate; this leads to loss of their ability to degrade pollutants. The ZVI with stable structure and high specific surface area is expected.

Obviously, the micro/nanostructured particles would prevent agglomeration and possess the structural stability of the bulk and the high activity of the nanoparticles.[28,29] Thus, the ZVI particles with this micro/nanostructure can be a better candidate material to effectively remove Cr(VI). In this study, plate-like micro/nanostructured zero-valent iron (MNZVI) prepared by ball-milling the industrially reduced iron powders is used for the removal of Cr(VI) from aqueous solutions based on chemical reduction. This MNZVI has demonstrated significantly higher ability to remove Cr(VI) than commercial zero valent iron (CZVI) from aqueous solutions. The reaction rate constant for MNZVI is 20 times larger than that for CZVI. Furthermore, the experiments in real electroplating wastewater have demonstrated that MNZVI has a good practical application potential for the treatment of Cr(VI)-containing wastewater. The details have been reported herein.

2. Experimental

2.1. Preparation of plate-like MNZVI

Plate-like MNZVI was prepared by ball-milling the industrially reduced iron powders. Briefly, the industrially oxidized iron scale was reduced into iron powders at 650 °C under a H_2 atmosphere that were subsequently passed through a 320-mesh sieve. The passed iron powders were then ball-milled for about 120 h in a ball mill by steel balls (ϕ 5–10 mm) under 7.5 kW power at room temperature. For avoiding oxidation and convenient storage, stearic acid was added according to the ratio of stearic acid to reduced iron powders of 1 : 10 (or 1 g stearic acid was added to 10 g reduced iron powders) during the ball milling process. After ball milling and drying at 60 °C, stearic acid-coated MNZVI was obtained, subsequently soaked in a 4 M NaOH solution, and shaken at 200 rpm for 1 h. It was then taken out and washed with deionized water and ethanol several times to remove stearic acid from MNZVI. Finally, MNZVI was dried in a vacuum oven at 60 °C before characterization or use for the Cr(VI) removal experiment.

For reference, commercial zero valent iron (CZVI) powders (size < 100 mesh, Fe: >98%) were purchased from Beijing Chemical Factory, China. The ball-milled iron and CZVI powders were characterized by field emission scan electron microscopy (FESEM, Sirion 200 U.S.A.) and X-ray diffraction (XRD, Philips X'Pert Pro MPD) with Cu Kα radiation (1.5406 Å). Fourier transform infrared (FTIR) spectroscopy was performed *via* an infrared spectrophotometer (NEXUS, Thermo Nicolet Corporation) using the KBr pellet technique in the range of 400–4000 cm^{-1}. X-ray photoelectron spectroscopic (XPS) analyses were carried out using a Thermo ESCALAB 250 analyzer. An Al Kα X-ray source ($h\nu$ = 1486.6 eV) was operated with a pass energy of 20 eV. The isothermal N_2 sorption was measured using a gas sorption apparatus (Omnisorp 100 CX, Coulter, U.S.A.), and a quartz tube with the sample was heated in the apparatus to 300 °C in vacuum for outgassing before measurement of N_2 isothermal sorption at the liquid nitrogen temperature.

2.2. Batch experiments

Sodium hydroxide (NaOH), ethanol (C_2H_5OH), potassium dichromate ($K_2Cr_2O_7$), and hydrochloric acid (HCl) were obtained from National Medicines Co. Ltd. of China with analytical grade and used as received without further purification.

At first, an aqueous solution with 100 ppm Cr(VI) was prepared by dissolving $K_2Cr_2O_7$ in deionized water. Then, 30 mg as-prepared MNZVI or as-purchased CZVI was added to the 20 mL Cr(VI)-containing aqueous solution. The pH in the solution was adjusted to 2 using HCl or Na(OH). A series of identical or parallel samples with ZVI were prepared *via* this way. All the parallel samples were placed in a constant temperature shaker and shaken. After shaking for a certain interval, one of the samples was taken out, and 100 μL 2 M Na(OH) was then added to it to flocculate Cr(III) and iron ions in this sample. Moreover, the reaction in the solution of this sample would stop due to the alkaline condition. After being allowed to stand for 30 min, the reacted solution was separated by centrifugation, and the supernatant was used for measurement of the Cr(VI) content by an inductively coupled plasma emission spectrometer (ICP 6000). These procedures (sampling and alkali addition) were repeated at certain intervals. The pH values were measured using a Mettler Toledo pH meter (FG2/EL2).

3. Results and discussion

After ball milling, stearic acid-coated powders were obtained. The final products were thus acquired *via* subsequent cleaning with a NaOH solution. FTIR spectral measurements show that stearic acid on the powder surface has been removed, as illustrated in Fig. S1.† FESEM observation has revealed that the cleaned ball-milled iron powders consist of plate-like particles 3–10 μm in the planar dimension and smaller than 200 nm in thickness, as shown in Fig. 1(a). Fig. 1(b) shows the corresponding XRD pattern, which exhibits the broad diffraction peaks typical of a material with poor crystallinity. All the peaks can be indexed to the bcc structure of pure iron with the lattice constants of $a = b = c = 2.8608$ Å (JCPDS no. 87-0722). The poor crystallinity is attributed to the ball milling-induced high deformation in the plate-like MNZVI's surface layer. Furthermore, the specific surface area of this MNZVI is estimated to be

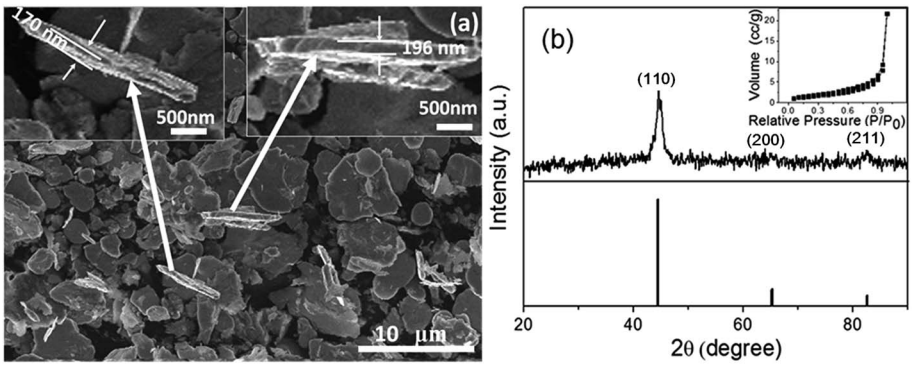

Fig. 1 Morphology and phase structure of the as-ball milled iron powders; (a) FESEM image. The insets: the magnified images of two single plates. (b) The XRD pattern of the plates. The line spectrum is the standard diffraction of the pure iron powders. The inset: N_2 isotherms.

about 15.1 $m^2\ g^{-1}$ by isothermal nitrogen sorption measurements, as illustrated in the inset of Fig. 1(b). This is much higher than that of the CZVI powders, which consists of the equi-axial pure iron particles (about 100 μm in size), sharp peaks in XRD pattern, and 0.5 $m^2\ g^{-1}$ specific surface area, as shown in Fig. S2(a–c).†

3.1. Cr(VI) removal

When this plate-like MNZVI was added to the Cr(VI)-containing aqueous solution the reaction took place. The solution gradually changed from yellow to colorless during the reaction, as typically illustrated in Fig. S3(a and b).† When a sample was taken out from the shaker after a certain interval, the flocculant (NaOH) was added to it. The reaction solution would thus produce light-green floc, as shown in Fig. S3(c),† indicating the existence of Fe(II) and/or Cr(III) induced by a redox reaction. This meant that some Cr(VI) could have been reduced to Cr(III) by ZVI during the reaction. This floc was subsequently removed by centrifugation separation [Fig. S3(d)†]. The residual Cr(VI) in the reacted solution was thus measured. Curve (I) in Fig. 2(a) shows the corresponding Cr(IV) content in the contaminated solution with 100 ppm initial Cr(IV) content wand 30 mg MNZVI addition amount as a function of the reaction time. It can be seen that Cr(VI) is completely removed in 18 min. Correspondingly, the pH value in the solution increased from 2.0 to 6.3. Conversely, for the addition of CZVI, the removal percentage of Cr(VI) is only 23% for the same reaction time, as shown in curve (II) of Fig. 2(a) and the pH value in the solution slightly increases from 2.0 to 3.2 [see Fig. 2(a)].

Further, the time-dependent Cr(VI) removal, as shown in Fig. 2(a), can be quantitatively described by the pseudo first-order reaction[30] or

$$\ln\frac{C}{C_0} = -k_{obs}t \quad (1)$$

$$k_{obs} = k_{SA}a_s\rho_m \quad (2)$$

where C_0 and C are the Cr(VI) content (mg L^{-1}) before and after the reaction time t. k_{obs} is the observed reaction rate constant (min^{-1}), which is the product of three parameters: k_{SA} is the specific reaction rate constant (L h^{-1} m^2), a_s is the specific surface area ($m^2\ g^{-1}$), and ρ_m is the mass concentration (g L^{-1}). In other words, the plot of $\ln\frac{C}{C_0}$ *versus* the reaction time t should

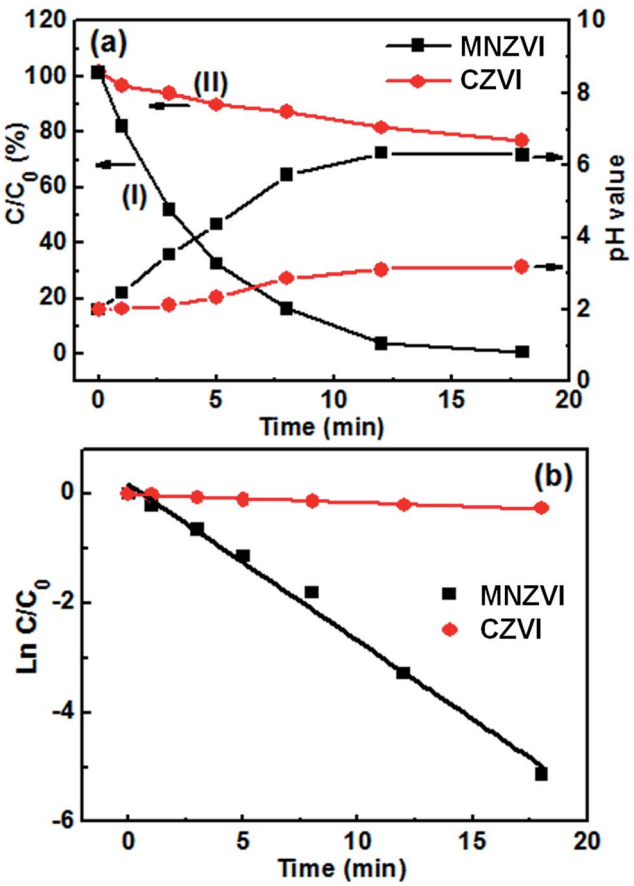

Fig. 2 The time-dependent Cr(VI) removal in the solutions with the additions of MNZVI and CZVI. (The initial Cr(VI) content: 100 ppm; the ZVI dosage: 1.5 g L^{-1}; and the initial pH = 2) (a) Cr(VI) content and pH values in the solutions as a function of the reaction time. (b) Plots of $\ln\frac{C}{C_0}$ *vs.* the reaction time [data from (a)]. Straight lines are the fitting results according to eqn (1).

be a straight-line. Fig. 2(b) shows the corresponding results and exhibits a very good linear relation between $\ln\frac{C}{C_0}$ and the time t within 20 min. The correlation coefficients are higher than 0.99. Obviously, the pseudo first-order kinetics is valid during the whole reaction period for the zero valent iron-based Cr(VI) removal. The reaction rate constants k_{obs} are thus estimated to be 0.286 and 0.0147 min^{-1} for the addition of MNZVI and CZVI, respectively. The reaction rate constant for the former is about 20 times higher than that for the latter and 10 times higher than the previously reported value [0.0275 min^{-1}].[31]

3.2. Influencing factors

Further experiments have revealed that the initial pH value and ZVI loading amount in the solution are also important for the Cr(VI) removal.

3.2.1. The initial pH value. The existence form of Cr(VI) depends on the pH value in the aqueous solution. Cr(VI) exists mainly in the form of $Cr_2O_7^{2-}$ when the pH value falls in the range from 1.0 to 6.0, whereas it exists in the form of CrO_4^{2-} when pH is higher than 6.0.[31–33] Thus, the initial pH value in the solutions would influence the reduction reaction of Cr(VI) by ZVI. Fig. 3 shows the effect of the initial pH value on the removal rate of Cr(VI) in the solution within 20 min. The time-dependent Cr(VI) removal at different initial pH values can also be well described by eqn (1), as illustrated in Fig. S4.† The corresponding reaction rate constants k_{obs} for the addition of MNZVI are thus obtained, as shown in Fig. 3. It has been demonstrated that the Cr(VI) removal rate within 20 min and the corresponding k_{obs} values decrease sharply with an increase in the initial pH value from 2 to 3.5. When the pH value is higher than 3.5, however, the Cr(VI) removal rates within 20 min are below 10% and remain almost unchanged with the increasing initial pH value; moreover, the k_{obs} values are very small (0.003 min^{-1}), as shown in Fig. 3. Obviously, the low initial pH condition below 3.5 is beneficial for the Cr(VI) removal with a high efficiency. For the addition of CZVI, similar evolution was observed, but the values of Cr(VI) removal rate were much lower, as demonstrated in Fig. 3.

3.2.2. ZVI dosage. Finally, the effect of ZVI dosage on Cr(VI) removal was studied. Fig. 4 presents the corresponding results of the Cr(VI) removal rate within 20 min as a function of the addition amounts of MNZVI and CZVI for the aqueous solution with 100 ppm initial Cr(VI) content. The Cr(VI) removal rate nearly linearly increases up to 100% with the increasing MNZVI dosage up to 1.5 g L^{-1}. For CZVI, however, the Cr(VI) removal rate increases only gradually with the increasing addition amount. Even when the dosage is up to 5 g L^{-1}, the removal rate is still below 30% under our experimental conditions. It is evident that plate-like MNZVI has much higher efficiency than CZVI for the removal of Cr(VI).

3.3. Adsorption and reduction-induced Cr(VI) removal

Herein, the mechanism of Cr(VI) removal by ZVI has been briefly discussed, which can be attributed to Cr(VI) adsorption on the iron particle surface and reduction reaction. When MNZVI or CZVI was added to the Cr(VI)-containing solutions at a low initial pH value, the Cr(VI) or $Cr_2O_7^{2-}$ adsorption occurred on the solid iron surface and then induced a reduction reaction as follows:[34]

$$3Fe^0 + Cr_2O_7^{2-} + 14H^+ \rightarrow 3Fe^{2+} + 2Cr^{3+} + 7H_2O \quad (3)$$

i.e. the Fe^0 atoms on the MNZVI object surface would react with the adsorbed Cr(VI) or $Cr_2O_7^{2-}$, producing Cr(III) and Fe^{2+}ions, as schematically demonstrated in Fig. 5(a). On the other hand, the formed Fe^{2+} ions could also reduce Cr(VI) to Cr(III) and form Fe^{3+} ions according to the following reaction:[34]

$$6Fe^{2+} + Cr_2O_7^{2-} + 14H^+ \rightarrow 6Fe^{3+} + 2Cr^{3+} + 7H_2O \quad (4)$$

as illustrated in Fig. 5(b). Subsequently, *via* the addition of NaOH to the reacted solution, the flocculation reaction took place. Cr(III) and Fe^{3+} ions produced in the reacted solution according to the reactions (3) and (4) were thus removed due to

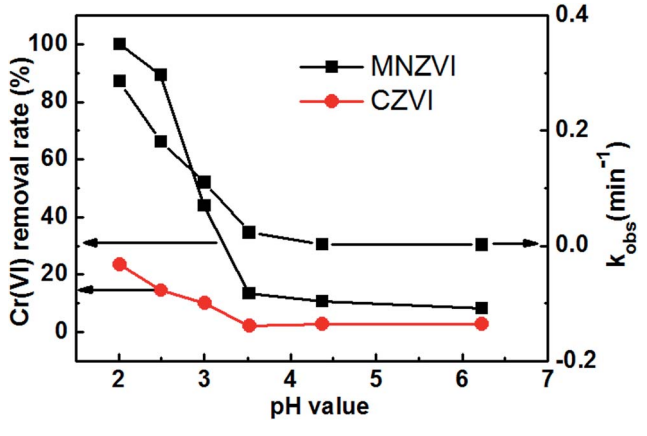

Fig. 3 Effects of the initial pH value on the Cr(VI) removal rates and reaction rate constants k_{obs} after reaction for 18 min (the initial Cr(VI) content: 100 ppm; the ZVI dosage: 1.5 g L^{-1}).

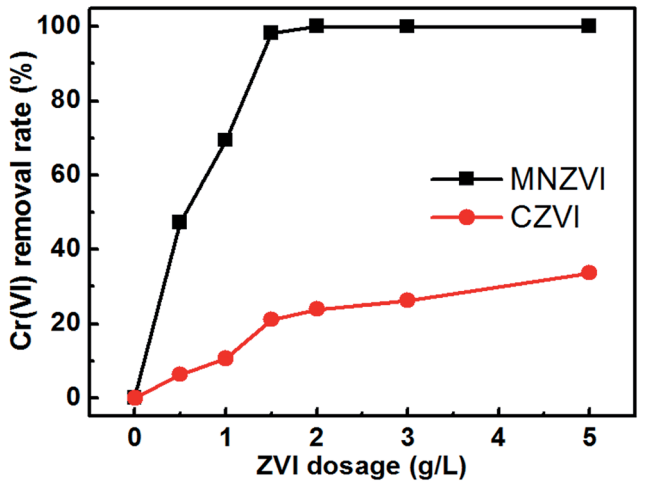

Fig. 4 Effects of the ZVI dosage on the Cr(VI) removal rate after reaction for 18 min in the solution with 100 ppm initial Cr(VI) content.

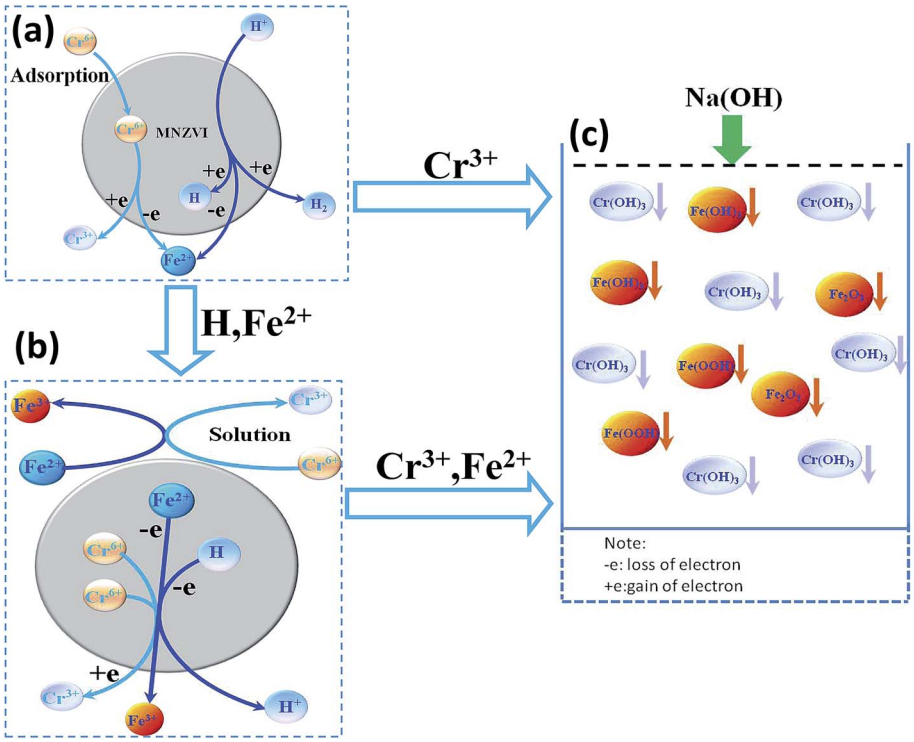

Fig. 5 Schematic of the plate-like MNZVI-induced Cr(VI) removal. (a) Adsorption and reduction reaction of $Cr_2O_7^{2-}$ ions on the plate-like MNZVI. (b) Fe^{2+} ions-induced reduction of the $Cr_2O_7^{2-}$ ions; and (c) Cr removal from the solution by flocculation.

the formation of chromium and iron hydrates (or oxides)[35] according to reactions (5) and (6), as shown in Fig. 5(c); this led to the final removal of Cr(VI) from the solution.

$$Fe^{3+} + 3OH^- \rightarrow Fe(OH)_3\downarrow \quad (5)$$

$$Cr^{3+} + 3OH^- \rightarrow Cr(OH)_3\downarrow \quad (6)$$

For confirmation, the XPS measurements were conducted for MNZVI after its immersion in the Cr(VI)-containing solution for 18 min, as illustrated in Fig. S5(a).† It has been shown that chromium adsorbed on the plate-like MNZVI surface is mainly Cr(III), therefore indicating the occurrence of reduction of Cr(VI) to Cr(III). It has also been confirmed that the Fe content in the MNZVI-added solution increases with the reaction time, as demonstrated in Fig. S5(b);† this indicates the continuous dissolution or oxidation of zero valent iron during the reaction [see the reactions (3) and (4)]. Correspondingly, XRD was also conducted for the plate-like MNZVI after the reaction, as shown in Fig. S6.† All diffraction peaks were still ascribed to pure iron, but became sharper than those obtained before the reaction, thus showing better crystallinity. This is attributed to the reaction-induced removal or dissolution of the MNZVI surface layer, which is highly deformed due to ball milling.

Based on the abovementioned discussion, the enhanced Cr(VI) removal performance of plate-like MNZVI can be easily understood. There exist active sites on the iron particles.[36] These active sites could not only adsorb Cr(VI) in the aqueous solution, but also produce Fe^{2+} at a low pH by reaction with H^+ ions; this promoted the reduction of Cr(VI) according to the reactions (3) and (4). Compared with the CZVI powders, MNZVI has many more active sites due to the higher specific surface area and hence shows much higher and faster Cr(VI) removal performance, as demonstrated in Fig. 2. Similarly, since the number of active sites increases with the increasing ZVI dosage, the Cr(VI) removal performance increases with the increasing ZVI dosage (Fig. 4). Moreover, according to the reactions (3) and (4), the reduction reaction would consume H^+ ions and hence increase the pH value of the reaction solution (Fig. 2(a)). With regard to the effect of the initial pH values in the solution, as observed from the reactions (3) and (4), the low pH value would promote the reduction reaction of Cr(VI) and hence Cr(VI) removal (Fig. 3).

3.4. Application in a real electroplating wastewater

Further, plate-like MNZVI was used for the treatment of real electroplating wastewater. Briefly, the real electroplating wastewater was obtained from Xinming Electroplating Factory in Hefei, China. In the wastewater, the pH value was ~1.85, and Cr content was about 5373 ppm, in which Cr(III) was about 5% of the total Cr content (or 268.7 ppm), as measured by precipitating Cr(III) as $Cr(OH)_3$.[37] In addition to Cr, there also exist iron ions (0.8%), copper ions (2.6%), and SO^{4-} ions in this electroplating wastewater. This wastewater was first diluted into solutions with different Cr(VI) contents. The pH value is kept at about 2. Then, 20 mg MNZVI or CZVI was added to 20 mL solutions with different Cr(VI) contents. After the reaction proceeded for 1 h, 100 μL 2 M Na(OH) was added to the reacted

solutions for the flocculation of Cr(III) and iron ions. After standing for 60 min, the samples were separated by centrifugation, and the Cr(VI) content in the supernatant was measured. Herein, we defined the removal capacity Q_r as follow:

$$Q_r = (C_0 - C_r)\frac{V}{M} \quad (7)$$

where Q_r is the Cr(VI) amount removed by a unit mass of ZVI, C_0 and C_r are the contents of Cr(VI) before and after reaction, respectively, V is the solution volume, and M is the ZVI dosage.

Fig. 6(a) shows the removal capacity (Q_r) as a function of the initial Cr(VI) content in the electroplating wastewaters for the addition of MNZVI and CZVI. The removal capacity increases with the increasing initial Cr(VI) content, but tends to saturate when the initial content is up to near 600 ppm for the addition of MNZVI and near 300 ppm for the addition of CZVI. The measured maximum removal capacity was up to 330 mg g^{-1}, corresponding to the initial Cr(VI) content of 556 ppm for the addition of MNZVI, which was much higher than that for the addition of CZVI (only 94 mg g^{-1}). Moreover, this removal capacity is significantly higher than the previously reported results (up to 182.8 mg g^{-1}) obtained using nanoscaled ZVI or nanocomposites[2,27,38,39] and very close to that (up to 344.8 mg g^{-1}) obtained using FeO–rGO (reduced graphene oxide) composites.[40] Comparatively, the plate-like MNZVI in this study is more cost-effective.

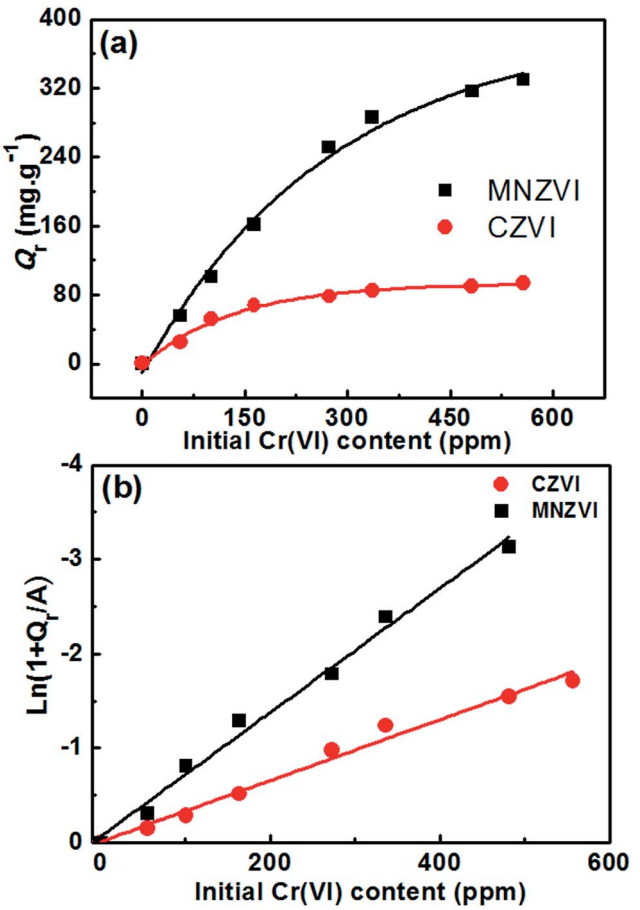

Fig. 6 (a) The removal capacity (Q_r) as a function of the initial Cr(VI) content in the electroplating wastewaters for the additions of MNZVI and CZVI; (b) the plots of $\ln\left(1+\frac{Q_r}{A}\right)$ *versus* C_0. The A values are −401.1 mg g^{-1} and −95.2 mg g^{-1} for the additions of MNZVI and CZVI, respectively, which are obtained by fitting the data in (a) according to eqn (8).

Furthermore, it was found that the dependence of the removal capacity (Q_r) on the initial Cr(VI) content (C_0) could be well described by the following empirical relation:

$$Q_r = A[\exp(BC_0) - 1] \quad (8)$$

where A and B are the constants independent of the initial Cr(VI) content C_0 (in ppm). By fitting, the parameters A and B were estimated to be −401.1 mg g^{-1} and −0.0036 ppm^{-1} for the addition of MNZVI and −95.2 mg g^{-1} and −0.0073 ppm^{-1} for the addition of CZVI, respectively. In this case, the plots of $\ln\left(1+\frac{Q_r}{A}\right)$ *versus* C_0 should be straight lines, which are in good agreement with our results illustrated in Fig. 6(b). Both exhibit good straight lines (the correlation coefficients are >0.99 for both).

As abovementioned, the high removal capacity for plate-like MNZVI could be associated with its high surface area or more active sites as compared to that of CZVI. The increase in the removal capacity with the increasing initial Cr(VI) content can be easily understood. Herein, the removal capacity Q_r is defined as the Cr(VI) amount removed by a unit mass of ZVI in 60 min based on eqn (7). Obviously, in the contaminated solution with a higher initial Cr(VI) content, the removal amount would be larger within the same reaction duration (or 1 h) due to faster Cr(VI) adsorption on the ZVI, or *vice versa*. It means that in the contaminated solution with a relatively low Cr(VI) content, the reaction time should be longer.

4. Conclusions and remarks

In summary, ball-milling induced plate-like MNZVI has been successfully used for the removal of Cr(VI) from aqueous solutions under an acidic condition. Cr(VI) could be removed nearly completely from the 100 ppm Cr(VI)-containing solution at pH = 2 within 20 min by the addition of 1.5 g L^{-1} plate-like MNZVI, thus showing significantly enhanced removal performance as compared to CZVI. The time-dependent removal amount of Cr(VI) was subject to a pseudo first-order kinetic model. The reaction rate constant for the MNZVI is 20 times larger than that for CZVI. The excellent removal performance of MNZVI could be attributed to the iron-induced reduction process of Cr(VI) and its high specific surface area. Importantly, this MNZVI has exhibited promising practical application in the treatment of real electroplating wastewaters. The removal capacity of MNZVI can reach up to 330 mg g^{-1} in a real electroplating wastewater, which is more than 3 times higher than that of CZVI and much higher than the previously reported results.

It should be mentioned that ZVI is disposable in the treatment of Cr(VI)-contaminated water. The addition of ZVI to the

Cr(VI)-containing solution induces the reduction of Cr(VI) to Cr(III) and dissolution of the added ZVI in the solution. Thus, the finally obtained products (after flocculation) contain mainly ferric and chromium oxides. These obtained products are thus not reusable. Fortunately, plate-like MNZVI can be mass-produced and is hence cost-effective. Moreover, the over-dosage of MNZVI could induce faster Cr(VI) removal, whereas the lower dosage would decrease the cost for practical applications. However, a longer time would be needed. This study has demonstrated that the plate-like MNZVI is a good candidate material for the efficient treatment of the Cr(VI)-containing wastewater.

Conflicts of interest

There are no conflicts to declare.

Acknowledgements

This work was financially supported by the National Key Basic Research Program of China (Grant No. 2013CB934303) and the CAS/SAF International Partnership Program for Creative Research Teams.

References

1 X. L. Tan, M. Fang, X. M. Ren, H. Y. Mei, D. D. Shao and X. K. Wang, *Environ. Sci. Technol.*, 2014, **48**, 13138–13145.
2 X. S. Lv, J. Xu, G. M. Jiang, J. Tang and X. H. Xu, *J. Colloid Interface Sci.*, 2012, **369**, 460–469.
3 J. Lv, W. B. Jiao, H. Y. Qiu, B. Chen, X. X. Huang and B. Kang, *Geoderma*, 2018, **310**, 99–106.
4 H. J. Su, Z. Q. Fang, P. E. Tsang, L. C. Zheng, W. Cheng, J. Z. Fang and D. Y. Zhao, *J. Hazard. Mater.*, 2016, **318**, 533–540.
5 P. Mitra, D. Sarkar, S. Chakrabarti and B. K. Dutta, *Chem. Eng. J.*, 2011, **171**, 54–60.
6 J. M. Chen and O. J. Hao, *Crit. Rev. Environ. Sci. Technol.*, 1998, **28**, 219–251.
7 H. Yoshitake, T. Yokoi and T. Tatsumi, *Chem. Mater.*, 2002, **14**, 4603–4610.
8 J. W. He, Y. Long, Y. Y. Wang, C. L. Wei and J. J. Zhan, *ACS Appl. Mater. Interfaces*, 2016, **8**, 16699–16707.
9 J. W. Patterson, E. Gasca and Y. Wang, *Water Sci. Technol.*, 1994, **29**, 275–284.
10 M. J. McGuire, N. K. Blute, C. Seidel, G. Qin and L. Fong, *J. - Am. Water Works Assoc.*, 2006, **98**, 134–143.
11 A. Agrawal, V. Kumar and B. D. Pandey, *Miner. Process. Extr. Metall. Rev*, 2006, **27**, 99–130.
12 A. Naghizadeh, *J. Water Supply Res. T.*, 2015, **64**, 64–73.
13 R. S. Bowman, *Microporous Mesoporous Mater.*, 2003, **61**, 43–56.
14 S. Guha and P. Bhargava, *Water Environ. Res.*, 2005, **77**, 411–416.
15 M. S. Gasser, G. A. Morad and H. F. Aly, *J. Hazard. Mater.*, 2007, **142**, 118–129.
16 T. Z. Liu and I. M. C. Lo, *Water, Air, Soil Pollut.*, 2011, **216**, 473–483.
17 S. C. N. Tang, K. Yin and I. M. C. Lo, *J. Contam. Hydrol.*, 2011, **125**, 39–46.
18 N. Moraci and P. S. Calabro, *J. Environ. Manage.*, 2010, **91**, 2336–2341.
19 M. Powell, R. W. Puls, S. K. Hightower and D. A. Sabatini, *Environ. Sci. Technol.*, 1995, **29**, 1913–1922.
20 X. T. Liu, W. Zhao, K. Sun, G. X. Zhang and Y. Zhao, *Chemosphere*, 2011, **82**, 773–777.
21 S. L. Li, W. Wang, F. P. Liang and W. X. Zhang, *J. Hazard. Mater.*, 2017, **322**, 163–171.
22 L. Santos-Juanes, F. S. G. Einschlag, A. M. Amat and A. Argues, *Chem. Eng. J.*, 2017, **310**, 484–490.
23 R. B. Fu, X. Zhang, Z. Xu, X. P. Guo, D. S. Bi and W. Zhang, *Sep. Purif. Technol.*, 2017, **174**, 362–371.
24 B. Sunkara, J. J. Zhan, J. B. He, G. L. McPherson, G. Piringer and V. T. John, *ACS Appl. Mater. Interfaces*, 2010, **2**, 2854–2862.
25 Q. Wang, N. Cissoko, M. Zhou and X. H. Xu, *Phys. Chem. Earth*, 2011, **36**, 442–446.
26 X. B. Zhou, B. H. Lv, Z. M. Zhou, W. X. Li and G. H. Jing, *Chem. Eng. J.*, 2015, **281**, 155–163.
27 Z. Q. Fang, X. Q. Qiu, R. X. Huang, X. H. Qiu and M. Y. Li, *Desalination*, 2011, **280**, 224–231.
28 X. B. Wang, W. P. Cai, G. Z. Wang, Z. K. Wu and H. J. Zhao, *CrystEngComm*, 2013, **15**, 2956–2965.
29 S. W. Liu, S. H. Kang, G. Z. Wang, H. J. Zhao and W. P. Cai, *J. Colloid Interface Sci.*, 2015, **458**, 94–102.
30 L. N. Shi, X. Zhang and Z. L. Chen, *Water Res.*, 2011, **45**, 886–892.
31 H. Zhou, Y. He, Y. Lan, J. Mao and S. Chen, *Chemosphere*, 2008, **72**, 870–874.
32 T. Lee, H. Lim, Y. Lee and J. W. Park, *Chemosphere*, 2003, **53**, 479–485.
33 D. Mohan and C. U. Pittman, *J. Hazard. Mater.*, 2006, **137**, 762–811.
34 Z. Y. Liang, Q. J. Wen, X. Wang, F. W. Zhang and Y. Yu, *Appl. Surf. Sci.*, 2016, **386**, 451–459.
35 X. Q. Li, J. S. Cao and W. X. Zhang, *Ind. Eng. Chem. Res.*, 2008, **47**, 2131–2139.
36 S. H. Kang, S. W. Liu, H. M. Wang and W. P. Cai, *J. Hazard. Mater.*, 2016, **307**, 145–153.
37 S. C. Xu, Y. X. Zhang, S. Wang, J. M. Xu, H. L. Ding and G. H. Li, *Eur. J. Inorg. Chem.*, 2013, 2601–2607.
38 A. K. Sharma, R. Kumar, S. Mittal, S. Hussain, M. Arora, R. C. Sharma and J. N. Babu, *RSC Adv.*, 2015, **5**, 89441–89446.
39 V. N. Montesinos, N. Quici, E. B. Halac, A. G. Leyva, G. Custo, S. Bengio, G. Zampieri and M. I. Litter, *Chem. Eng. J.*, 2014, **244**, 569–575.
40 X. S. Lv, Y. Qiu, Z. Y. Wang, G. M. Jiang, Y. T. Chen, X. H. Xu and R. H. Hurt, *Environ. Sci.: Nano*, 2016, **3**, 1215–1221.